

Article

Improving Effects of Laccase-Mediated Pectin–Ferulic Acid Conjugate and Transglutaminase on Active Peptide Production in Bovine Lactoferrin Digests

Mingxia Xing ^{1,†} , Ying Ji ^{1,†}, Lianzhong Ai ¹, Fan Xie ¹, Yan Wu ² and Phoency F. H. Lai ^{1,*} 

¹ Shanghai Engineering Research Center of Food Microbiology, School of Health Science and Engineering, University of Shanghai for Science and Technology, Shanghai 200093, China

² School of Agriculture and Biology, Shanghai Jiao Tong University, Shanghai 200240, China

* Correspondence: plai856@hotmail.com; Tel.: +86-18516077898

† These authors contributed equally to this work.

Abstract: Bovine lactoferrin (bLf) is a multifunctional glycoprotein and a good candidate for producing diverse bioactive peptides, which are easily lost during over-digestion. Accordingly, the effects of laccase-mediated pectin–ferulic acid conjugate (PF) and transglutaminase (TG) on improving the production of bLf active peptides by in vitro gastrointestinal digestion were investigated. Using ultra-high-performance liquid chromatography tandem mass spectroscopy (UPLC-MS-MS), the digests of bLf alone, PF-encapsulated bLf complex (LfPF), and TG-treated LfPF complex (LfPFTG) produced by conditioned in vitro gastric digestion (2000 U/mL pepsin, pH 3.0, 37 °C, 2 h) were identified with seven groups of active peptide-related fragments, including three common peptides (VFEAGRDPYKLRPVAEE, FENLPEKADRQYEL, and VLRPTEGYL) and four differential peptides (GILRPYLSWTE, ARSVDGKEDLIWKL, YLGSRYLT, and FKSETKNLL). The gastric digest of LfPF contained more diverse and abundant detectable peptides of longer lengths than those of bLf and LfPFTG. After further in vitro intestinal digestion, two active peptide-related fragments (FEAGRDPYK and FENLPEKADRQYE) remained in the final digest of LfPFTG; one (EAGRDPYKLRPVA) remained in that of bLf alone, but none remained in that of LfPF. Conclusively, PF encapsulation enhanced the production of bLf active peptide fragments under the in vitro gastric digestion applied. TG treatment facilitated active peptide FENLPEKADRQYE being kept in the final gastrointestinal digest.

Keywords: lactoferrin; pectin–ferulic acid conjugate; laccase; transglutaminase; active peptide; UPLC-MS-MS



Citation: Xing, M.; Ji, Y.; Ai, L.; Xie, F.; Wu, Y.; Lai, P.F.H. Improving Effects of Laccase-Mediated Pectin–Ferulic Acid Conjugate and Transglutaminase on Active Peptide Production in Bovine Lactoferrin Digests. *Catalysts* **2023**, *13*, 521. <https://doi.org/10.3390/catal13030521>

Academic Editors: Chia-Hung Kuo, Chwen-Jen Shieh and Hui-Min David Wang

Received: 31 December 2022

Revised: 20 February 2023

Accepted: 1 March 2023

Published: 3 March 2023



Copyright: © 2023 by the authors. Licensee MDPI, Basel, Switzerland. This article is an open access article distributed under the terms and conditions of the Creative Commons Attribution (CC BY) license (<https://creativecommons.org/licenses/by/4.0/>).

1. Introduction

Bovine lactoferrin (bLf) is a vital, multifunctional glycoprotein with diverse applications in foods [1] and pharmaceuticals [2]. It is a “generally recognized as safe” (GRAS) ingredient at a maximal usage of 100–400 mg/100 g for milk products [3]. For foods, bLf is a promising nutraceutical and encapsulating agent for functional ingredients [1]. For pharmaceuticals, bLf is a good candidate as an adjuvant or drug carrier in medicines such as antimicrobial, immunomodulatory, anticancer, anti-Parkinsonian, and anti-Alzheimer medicines [2,4]. For developing active peptides with improved activities, studies on bLf active peptides produced by in vitro gastric or gastrointestinal digestion are receiving more interest [5–9]. Several bLf active peptides have been discovered, e.g., antimicrobial peptides, bovine lactoferrampin (bLfampin) [5]; antihypertensive peptides, ENLPEKADR [6]; and osteoblast-promoting peptides, ENLPEKADRQYEL [7] and FKSETKNLL [8]. However, few pieces of evidence about whole active peptide distribution are reported for bLf digests, possibly due to over-digestion by the applied conditions or technical limitations for peptide identification [10].

Generally, enhancing active peptide production in bLf digests is essential for industrial concerns. For this purpose, several approaches for controlling bLf hydrolysis can be considered; examples include selecting suitable digestion conditions and encapsulation with food biopolymers. Natural pectins are multifunctional biopolymers widely applied in foods [11] and pharmaceuticals [12] and have potential for encapsulating bLf via electrostatic interactions [13,14]. Nonetheless, the encapsulation efficacy and stability of a bLf–natural pectin complex are limited [15] due to the high hydrophilicity of natural pectins. Recently, pectins have been receiving more interest for their ability to be conjugated with dietary phenolics (e.g., ferulic acid) [16–20], giving pectin–phenolic conjugates of improved hydrophobicity, solution viscosity, emulsion stability [16], and in vitro antioxidant activities [19,20]. In addition, a pectin–ferulic acid conjugate has been proven to encapsulate bLf better and give a lower particle size than its parent pectin [15]. The conjugate may be a good modulator for improving bLf active peptide production. However, the improvement remains to be proved.

Transglutaminase (TG), a popular modifier for food proteins [21], could be another choice for modulating bLf hydrolysis. The mechanism by which TG modifies protein functionality is well known to be the catalysis of an acyl transfer reaction between the γ -carboxamide group in the glutamine residue and a primary amine, usually in lysine residue, leading to the formation of γ -glutamyl-lysine (Gln-Lys) bonds and cross-links between polypeptides or proteins [21]. This type of crosslink has been proposed for TG-treated bLf particles that increased the stability of Pickering emulsions [22]. The potential of TG in modulating bLf active peptide production during digestion is still unclear and under investigation.

Accordingly, this study aimed to investigate the improving effects on bLf active peptide production under conditioned in vitro gastrointestinal digestion accomplished using two approaches: encapsulation of laccase-mediated pectin–ferulic acid conjugate (PF) and TG treatment. The study was performed from the viewpoint of digestomics with UPLC-MS-MS [10,23]. Passion fruit pectin (PP) was purposely applied for conjugation with ferulic acid, due to improved encapsulation ability toward bLf, giving the complex of significantly ($p < 0.05$) lessened effective particle sizes [15].

2. Results

2.1. Compositions and Characteristic Ratios of PP and PF

Table 1 indicates that PP possessed a total uronic acid content of 72.72% (w/w) on average, a total phenolic content (TPC) of 2.36 mg GAE/g, and a degree of esterification (DE) of 35.17%. In contrast to PP, PF showed a significantly ($p < 0.05$) lower total uronic acid content (63.19% (w/w)) but greater TPC (20.03 mg GAE/g) and DE (55.40%). For monosaccharide composition, PP was composed of GalA, Ara, Gal, Glc, and Rha at 53.42%, 14.73%, 18.50%, 9.11%, and 4.24%, respectively, in molar percentage. Comparatively, PF exhibited significantly ($p < 0.05$) lessened GalA (46.83%) and Rha (2.01%) compositions but heightened Glc% (16.02%). Five structural characteristic ratios for pectins were discovered. Homogalacturonan content (HG%) appeared to be 49.17% for PP, decreasing to 44.82% for PF. Rhamnogalacturonan type I composition (RG-I%) was estimated to be 41.72% for PP, slightly decreasing to 39.16% for PF. The ratio of GalA%/(Rha% + Ara% + Gal%), an index for structural linearity of the pectin chain, was 1.43 for PP, slightly lessening to 1.26 for PF. The ratio of Rha%/GalA%, an index for branching extent, was 0.08 for PP and was significantly reduced to 0.04 for PF. In addition, the ratio of (Ara% + Gal%)/Rha%, suggesting the side chain length of the RG-I fragment, was 7.87 for PP, significantly ($p < 0.05$) increasing to 17.53 for PF. FA seemed to bind selectively to the pectin molecules of the HG backbone with a low degree of branching and RG-I of long chain lengths.

Table 1. Approximate compositions, monosaccharide compositions, and ratios of PP and PF conjugates.

Parameter	Unit	PP	PF Conjugate
Total uronic acid content	(% w/w)	72.72 ± 2.53 ^{a,2}	63.19 ± 1.59 ^b
Total phenolic content (TPC)	(mg GAE/g) ¹	2.36 ± 0.01 ^b	20.03 ± 0.38 ^a
Degree of esterification (DE)	(%)	35.17 ± 1.04 ^b	55.40 ± 3.71 ^a
Monosaccharide composition			
Galacturonic acid (GalA)	(mol%)	53.42 ± 1.23 ^a	46.83 ± 0.64 ^b
Arabinose (Ara)	(mol%)	14.73 ± 0.18 ^a	15.16 ± 0.26 ^a
Galactose (Gal)	(mol%)	18.50 ± 1.28 ^a	19.98 ± 1.29 ^a
Glucose (Glc)	(mol%)	9.11 ± 0.27 ^b	16.02 ± 0.50 ^a
Rhamnose (Rha)	(mol%)	4.24 ± 0.32 ^a	2.01 ± 0.06 ^b
HG% = GalA% – Rha%	(mol%)	49.17 ± 1.46 ^a	44.82 ± 0.60 ^b
RG-I% = 2Rha% + Ara% + Gal%	(mol%)	41.72 ± 1.39 ^a	39.16 ± 0.92 ^a
GalA%/(Rha% + Ara% + Gal%)		1.43 ± 0.08 ^a	1.26 ± 0.05 ^a
Rha%/GalA%		0.08 ± 0.01 ^a	0.04 ± 0.00 ^b
(Ara% + Gal%)/Rha%		7.87 ± 0.59 ^b	17.53 ± 1.07 ^a

¹ GAE: gallic acid equivalent. ² Means ± standard deviations ($n = 3$); means with different superscripts a, b in the same row differ significantly ($p < 0.05$).

2.2. NMR-Evidenced Structural Features of PP and PF

Figure 1 presents ¹³C and ¹H-decoupled NMR spectra for structural identification of PP (A) and PF (B). Briefly, PP (Figure 1A) exhibited typical NMR signals of the HG backbone, accompanied by minor signals of RG-I branches, agreeing with its monosaccharide compositions (mainly ~49% HG% and partly ~42% RG-I of long-side-chain branches (Table 1)). According to our previous report [19] and those on passion fruit pectins [24] and pectic polysaccharides [25,26], the major peaks for PP could be assigned for the α-(1,4)-D-GalA residues of the HG backbone, where C1 δc = 100.40 ppm is associated with H1 δH = 5.03 ppm; C2 δc = 67.75 ppm with a shoulder peak C3 δc = 68.38 ppm, and both H2 and H3 δH = 3.75 ppm; C4 δc = 79.00 ppm, H4 δH = 3.94 ppm; C5 δc = 70.53 ppm, H5 δH ~ 5.05 ppm (associated with H1 δH); esterified carboxyl C6 δc = 170.67 ppm and free carboxyl C6 δc = 174.28 ppm (tiny peak), no δH; methoxyl C7 δc = 52.84 ppm, H7 δH ~ 3.75 ppm (coexisted with H2 and H3 δH); and Rha C6 δc = 16.51 ppm, δH = 1.16 ppm. In addition, tiny peaks at δc = 60.03, 71.27, 73–76, and 80–84 ppm could be attributed to branch Gal C6', Gal C5', Ara C3, and Ara C2 + C4, respectively. A peak at δc = 107.49 ppm was characteristic of terminal Ara C1 (t – A1) [25,26]. For the PF conjugate (Figure 1B), characteristic signals originating from FA were observed at δc = 43.71 ppm, δH = 2.69 and 2.82 ppm (-OCH₃ on phenyl ring), and δH = 7.45 and 7.51 ppm (parts of signals for methylene H on phenyl ring). The GalA C1 signal (originally δc = 100.37 ppm) likely shifted up to 98.00 ppm, accompanied by the other signals multiplied and of reduced intensities, possibly due to the shielding effect of bound FA. The above results confirm that FA is present in the PF conjugate, mostly via attaching to the nucleophilic carboxyl group of GalA residues. This kind of linkage is one of laccase-mediated FA redox reactions [18] and agrees with the evidence for citrus pectin–FA conjugates [17].

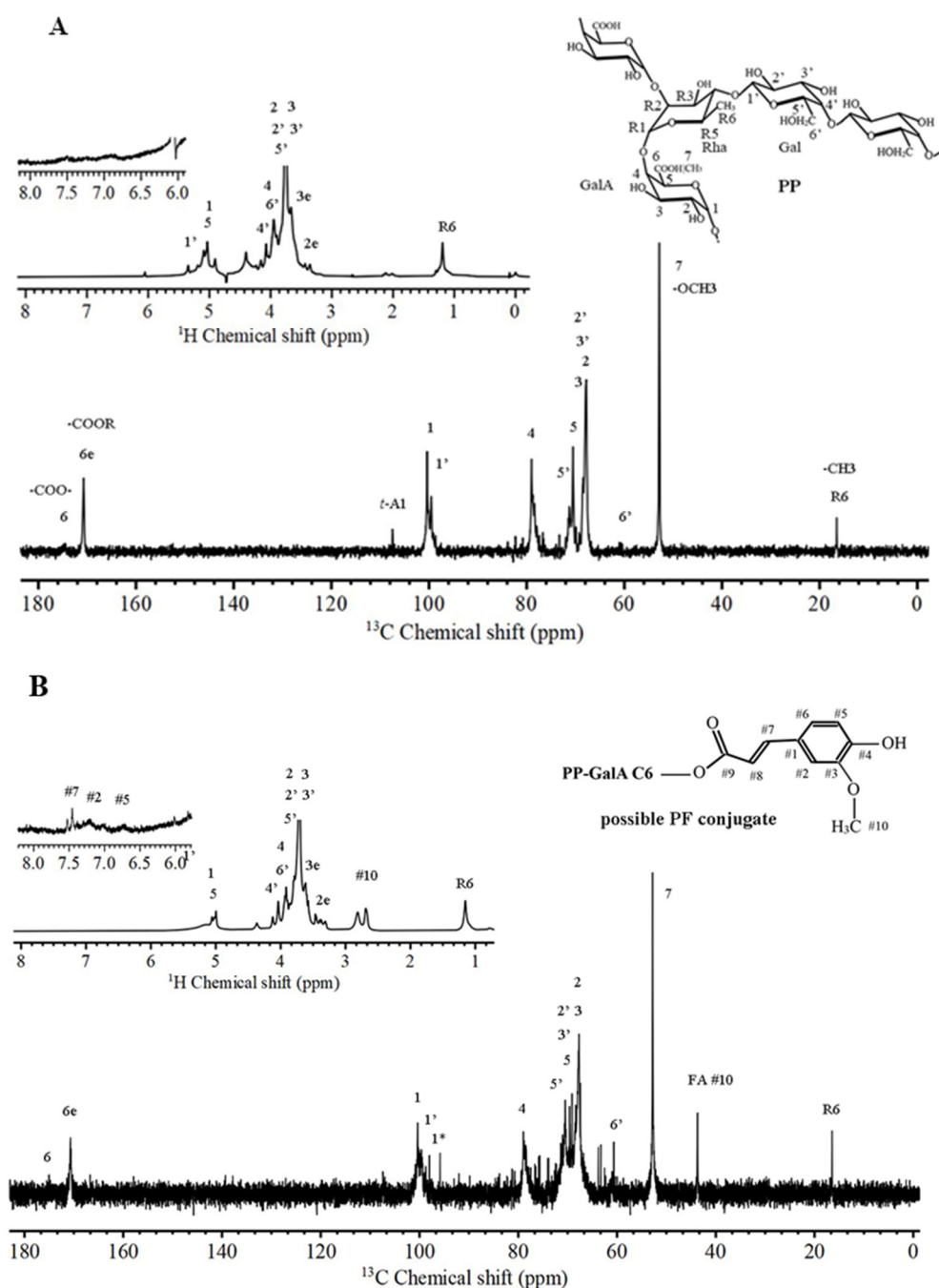


Figure 1. The 176 MHz ^{13}C and 700 MHz ^1H -decoupled NMR spectra of PP (A) and PF (B).

2.3. Particle Size Distributions of bLf, LfPF Complex, and LfPFTG Complex

Figure 2 shows that pure bLf aqueous solution (0.1% *w/w*) showed a bimodal distribution in particle size that peaked mainly at ~ 300 nm and minorly at ~ 2800 nm. After conjugation with PF, the LfPF complex (0.1% bLf + 0.025% PF) revealed a sharpened, bimodal distribution and shifted to small particle size regions, mainly peaking at 120 nm and associated with a small peak at ~ 25 nm. Additional treatment of 0.1% TG led to LfPFTG of a broad but monomodal distribution peaking at ~ 220 nm. The effective particle size and polydispersity index were, respectively, 269.1 ± 2.9 nm and 0.314 ± 0.076 for bLf alone, 157.0 ± 1.2 nm and 0.217 ± 0.006 for the LfPF complex, and 225.3 ± 7.3 nm and 0.231 ± 0.018 for the LfPFTG complex. In addition, the ξ -potential value was identified as $+21.9 \pm 0.42$ mV for the pure bLf dispersed solution, changing to -20.5 ± 1.69 mV for the LfPF complex, implying that negative-charge PF tended to cover positive-charge, spherical

bLf via electrostatic interactions. These changes are similar to those for a bLf complex with citrus low-methoxy pectin [14], which displayed a ξ -potential value (-43.6 mV) lower than that of LfPF [14] since that PF possessed a higher degree of esterification attributed to methoxy groups and esters formed between PP and FA (Figure 1). PF encapsulation on bLf was also confirmed by surface hydrophobicity and scanning electron micrograms [15].

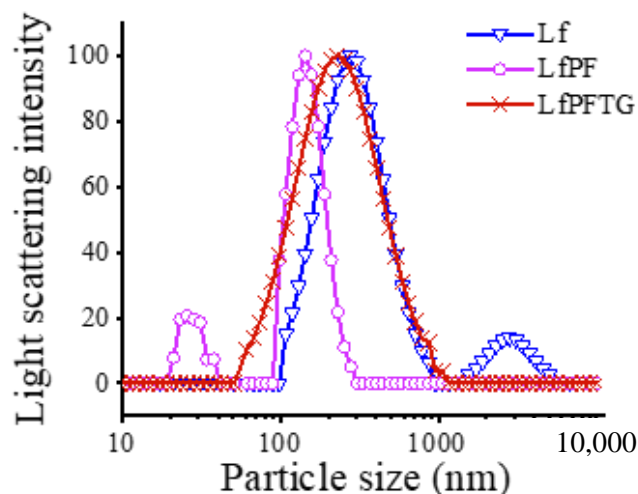


Figure 2. Particle size distributions of bLf, LfPF complex, and LfPFTG complex.

2.4. Differential Peptide Distributions after In Vitro Gastrointestinal Digestion

Figure 3 compares UPLC chromatograms for the peptide profiles in the digests of bLf, LfPF complex, and LfPFTG complex after in vitro gastrointestinal digestion. Obviously, in contrast to the chromatographic profile of bLf (A), those of in vitro gastric (pepsin) digests of LfPF (C) and LfPFTG (E) complexes were somewhat different. For the in vitro gastrointestinal (pepsin + trypsin) digests, the detected peak signals and peptide numbers lessened obviously in LfPFGI (D), but increased in LfPFTGGI (F), as compared with LfGI (B).

After MS-MS identification and homology matching with UniProt Knowledgebase (<https://www.uniprot.org/uniprotkb/P24627/entry>, accessed on 20 September 2022) and SWISS-MODEL (<https://swissmodel.expasy.org/>, accessed on 22 September 2022), the identified peptide fragments were tabulated (Supplementary Table S1). In total, there were 103 peptide fragments grouped into 19 peptide regions in the gastric digests studied (Table S2).

Briefly, the differential peptide numbers between samples are illustrated by Venn's plots (Figure 4). LfG, LfPFG, and LfPFTGG (Figure 4A) possessed total peptide numbers of 89, 91, and 77, respectively; individually, they possessed 4, 9, and 2 differential peptides, respectively, and they shared the same 66 peptides. There were 13, 6, and 3 same peptides between LfG and LfPFG, between LfG and LfPFTGG, and between LfPFG and LfPFTGG, respectively. For the gastrointestinal digests (Figure 4B), LfGI, LfPFGI, and LfPFTGGI contained total peptide numbers of only 7, 5, and 9, respectively; individually, they contained 4, 1, and 4 differential peptides, respectively, and they shared two same peptides. There were 0, 1, and 2 same peptides for LfGI vs. LfPFGI, LfGI vs. LfPFTGGI, and LfPFGI vs. LfPFTGGI, respectively.

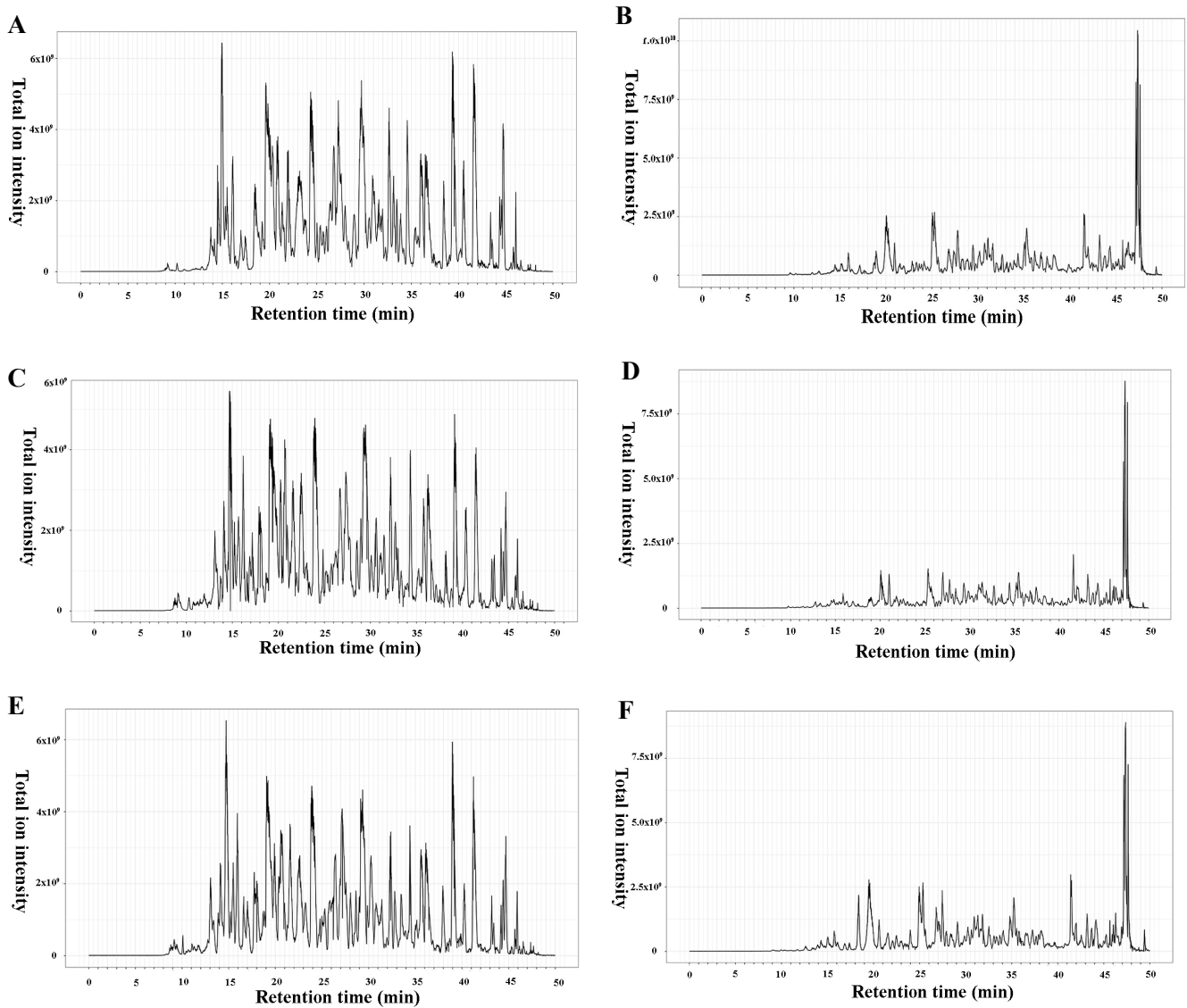


Figure 3. UPLC chromatograms for the peptide profiles in the digests of bLf (A,B), LfPF complex (C,D), and LfPFTG complex (E,F) after in vitro gastric (pepsin) digestion (A,C,E) and gastrointestinal (pepsin + trypsin) digestion (B,D,F).

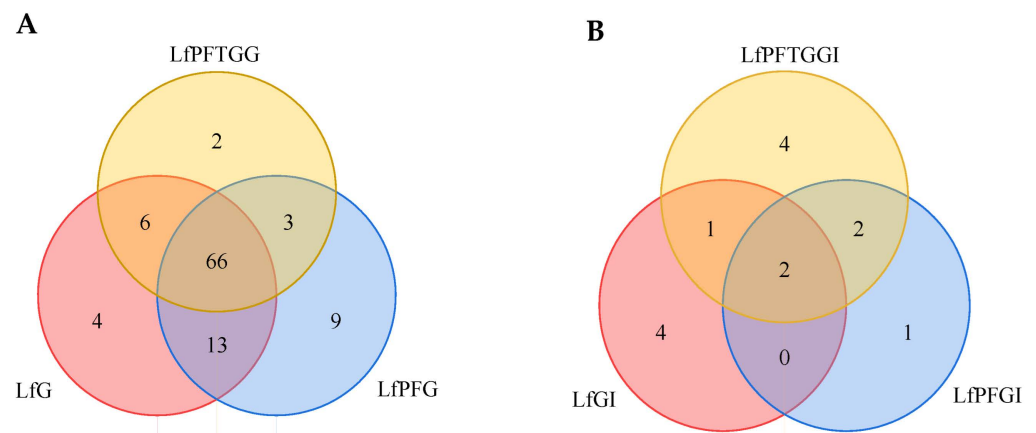


Figure 4. Venn's plots for differential peptide numbers detectable in the digests of bLf, LfPF complex, and LfPFTG complex after in vitro gastric digestion (A) and gastrointestinal digestion (B).

Figure 5 illustrates the histograms for peptide chain distributions detectable in the digests of bLf, LfPF, and LfPFTG by UPLC-MS-MS. The given LfG (A) showed detected peptide lengths in the range of 5–17 with abundances (number) topped at the lengths of 11–12, followed by 7–8. LfPFG (B) exhibited peptide lengths of 5–31 with abundance topped at 12, followed by 7–11. For LfPFTG (C), peptide lengths ranged from 6 to 16 with abundances maximized at 12, followed by 8. LfPFG exhibited high peptide abundance and long peptide chains (18–31) that were absent in both LfG and LfPFTGG. After further digestion by trypsin, the given LfGI (D), LfPFGI (E), and LfPFTGGI (F) displayed detectable peptide lengths in the ranges of 11–13, 7–14, and 6–16, respectively. Generally, total peptide abundance (peptide length \times number) followed the order of LfPFG > LfG and LfPFTGG; LfPFGI > LfPFTGGI > LfGI, agreeing with the order in total purified peptide yield examined by BCA colorimetric assay, generally 0.98% (*w/w*) for both LfG and LfPFTGG, 1.12% (*w/w*) for LfPFG, 0.29% (*w/w*) for LfGI, 0.44% (*w/w*) for LfPFGI, and 0.34% (*w/w*) for LfPFTGGI. The conjugation with PF and TG modified the detectable peptide chain distributions in bLf digests. Further treatment by *in vitro* intestinal digestion notably reduced the lengths and abundances of detectable peptides in the final digests. Peptides of very short lengths (<5 amino acid residues), long polypeptides (length > 31), and hetero-oligopeptides cross-linked by disulfide bonds were undetectable by high-resolution MS [27] and not indicated in this study.

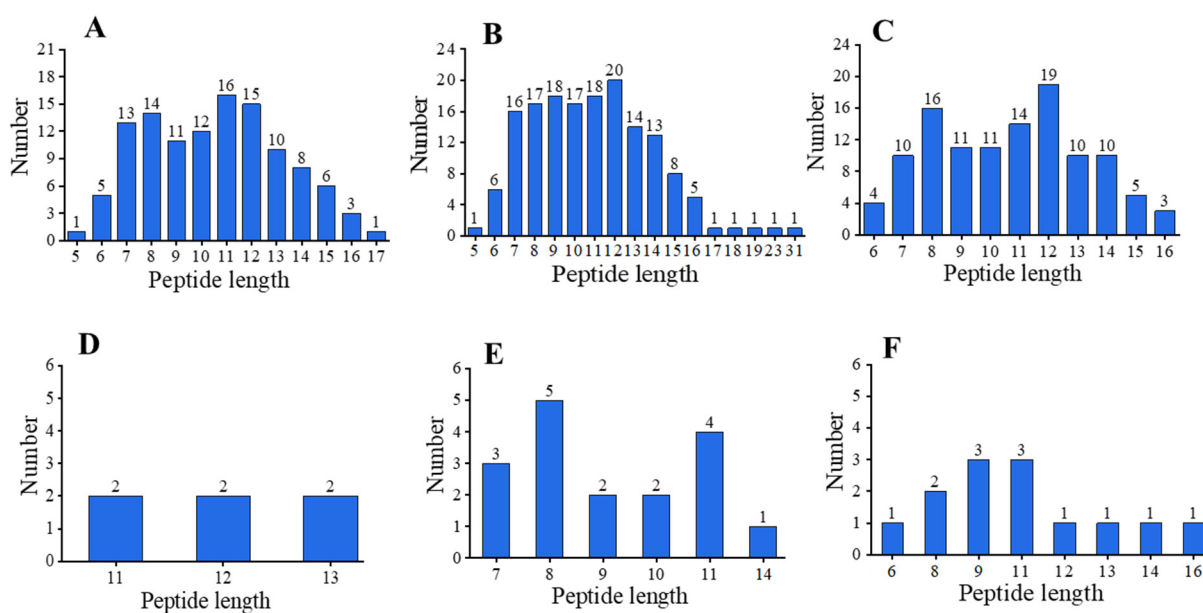


Figure 5. Detectable peptide profiles in the digests of bLf (A,D), LfPF complex (B,E), and LfPFTG complex (C,F) after *in vitro* gastric (pepsin) digestion (A–C) and gastrointestinal (pepsin + trypsin) digestion (D–F).

2.5. Differences in Active Peptide Fragments between Samples

Briefly, active peptide-related fragments are tabulated in Table 2; bioactive peptide sequences were determined from the milk bioactive protein database [28] and previous reports [5–9,29]. Seven groups of active peptide fragments with reported active peptide sequences were discovered in the gastric digests (LfG, LfPFG, and LfPFTGG): DG-GMVFEAGRDPYKLRPVAAE, f(79–99); GILRPYLSWTE, f(149–159); FENLPEKADRQYEL, f(234–248); ARSVDGKEDLIWKLLSK, f(276–292); YLGSRYLT, f(338–345); VLRPTEGYL, f(445–453); and LFKSETKNLL, f(650–659). For the final gastrointestinal digests, one active peptide type, EAGRDPYKLRPVA, f(85–97) and its related f(86–97), remained in LfGI. Two active peptides type, FEAGRDPYK, f(84–92), and FENLPEKADRQYE, f(234–247) and related f(235–246), were discovered in LfPFTGGI. No active peptides remained in LfPFGI.

Table 2. Active peptide fragments in the digests of bLf, LfPF complex, and LfPFTG complex produced by in vitro gastrointestinal digestion at pH 3.0.

Targeted Peptide Fragment	Peptide Fragment	Sequence	LfG	LfPF	Sample LfPFTGG	GI Digests
DGGMVFEAGRDPYKLRPVAAE, f(79–99)	VFEAGRDPYKLRPVAA	83–98	+	+	+	
	VFEAGRDPYKLRPVA	83–97	+	+	+	
	FEAGRDPYKLRPVAAE	84–99	+	+	+	
	FEAGRDPYKLRPVAA	84–98	+	+	+	
	FEAGRDPYKLRPVA	84–97	+	+	+	
	FEAGRDPYKLRPV	84–96	+	+	+	
	EAGRDPYKLRPVAAE	85–99	+	+	+	
	EAGRDPYKLRPVAA	85–98	+	+	+	
	EAGRDPYKLRPVA	85–97	+	+	+	LfGI (+)
	EAGRDPYKLRPV	85–96	+	+	+	
	AGRDPYKLRPVAAE	86–99	+	+	+	
	AGRDPYKLRPVAA	86–98	+	+	+	
	AGRDPYKLRPVA	86–97	+	+	+	LfGI (+)
	GRDPYKLRPVAA	87–98	+	+	+	
	GRDPYKLRPVA	87–97	+	+	+	
	RDPYKLRPVA	88–97	+	+	+	
	PYKLRPVA	90–97	+	+	+	
	YKLRPVA	91–97	+	+	+	
	AGRDPYKLRPV	86–96	+	+	+	
	PYKLRPVAAE	90–99	+	+	+	
	PYKLRPVAA	90–98	+	+	+	
	VFEAGRDPYKLRPV	83–96	+	+	+	
	EAGRDPYKLRP	85–95	+	+	+	
DGGMVFEAGRDPYKLRPVA	79–97	+	+	+		
VFEAGRDPYKLRPVAAE	83–99	+	+	+		
GRDPYKLRPV	87–96	+	+	+		
FEAGRDPYKLRP	84–95	+	+	+		
DPYKLRPVA	89–97	+	+	+		
GILRPYLSWTE, f(149–159)	GILRPYL	149–155	+	+	+	
	ILRPYLSW	150–157	+	+	+	
	ILRPYL	150–155	+	+	+	
	RPYLSWT	152–158	+	+	+	
	RPYLSWTE	152–159	+	+	+	
	RPYLSW	152–157	+	+	+	
	LRPYLSWT	151–158	+	+	+	
	LRPYLSW	151–157	+	+	+	
GILRPYLSW	149–157	+	+	+		
FENLPEKADRDQYEL, f(234–248)	FENLPEKADRDQYE	234–247	+	+	+	LfPFTGGI (+)
	FENLPEKADRDQ	234–245	+	+	+	
	ENLPEKADRDQYEL	235–248	+	+	+	
	ENLPEKADRDQYE	235–247	+	+	+	
	ENLPEKADRDQY	235–246	+	+	+	LfPFTGGI (+)
FENLPEKADRDQY	234–246	+	+	+		
ARSVDGKEDLIWKLLSK, f(276–292)	ARSVDGKEDLIWKL	276–289	+	+	+	
	RSVDGKEDLIWKL	277–289	+	+	+	
	RSVDGKEDLIWKLLSK	277–292	+	+	+	
	SVDGKEDLIWKLLSK	278–292	+	+	+	
YLGSRYLT, f(338–345)	YLGSRYLT	338–345	+	+	+	
	YLGSRYL	338–344	+	+	+	
VLRPTEGYL, f(445–453)	VLRPTEGYL	445–453	+	+	+	
	VLRPTEGY	445–452	+	+	+	
LFKSETKNLL, f(650–659)	FKSETKNLL	651–659	+	+	+	
	LFKSETKNLL	650–659	+	+	+	

2.6. bLf Active Peptide Changes during In Vitro Gastrointestinal Digestion

The effects of PF encapsulation and TG treatment on the resultant bLf active peptide profiles in the digests are differentiated as depicted in Figure 6. According to the results of molecular docking, it is suggested that bLf whatever alone or in LfPF and LfPFTG was generally digested by pepsin on the N1, N2, C1, and C2 termini, involving 6, 7, and 8 peptide regions, respectively (indicated by dashed red frames). The obtained pepsin

digests (LfG, LfPFG, and LfPFTGG) showed three common peptide fragments: f(83–99) (VFEAGRDPYKLRPVAAE), f(234–248) (FENLPEKADRDQYEL), and f(445–453) (VLRPT-EGYL). In addition, there were four differential peptides with lengths depending on the sample state: f(149–159) (GILRPYLSWTE), f(276–289) (ARSVDGKEDLIWKL), f(338–345) (YLGSRYLTL), and f(650–659) (LFKSETKNLL). After further intestinal (trypsin) digestion, LfGI contained peptide fragment f(85–97) (EAGRDPYKLRPVA). LfPFTGGI contained two active peptides, f(84–92) (FEAGRDPYK) and f(234–247) (FENLPEKADRDQYE). These results imply that the f(85–97) (EAGRDPYKLRPVA) fragment on the N1 terminus was quite resistant to *in vitro* gastrointestinal digestion. The presence of TG protected the peptide f(234–247) (FENLPEKADRDQYE) in the N2 terminus against *in vitro* gastrointestinal digestion. All active peptide fragments in the C1 and C2 termini were feasibly hydrolyzed during *in vitro* intestinal digestion and absent in the final digests, regardless of the protective effect of PF during *in vitro* gastric digestion.

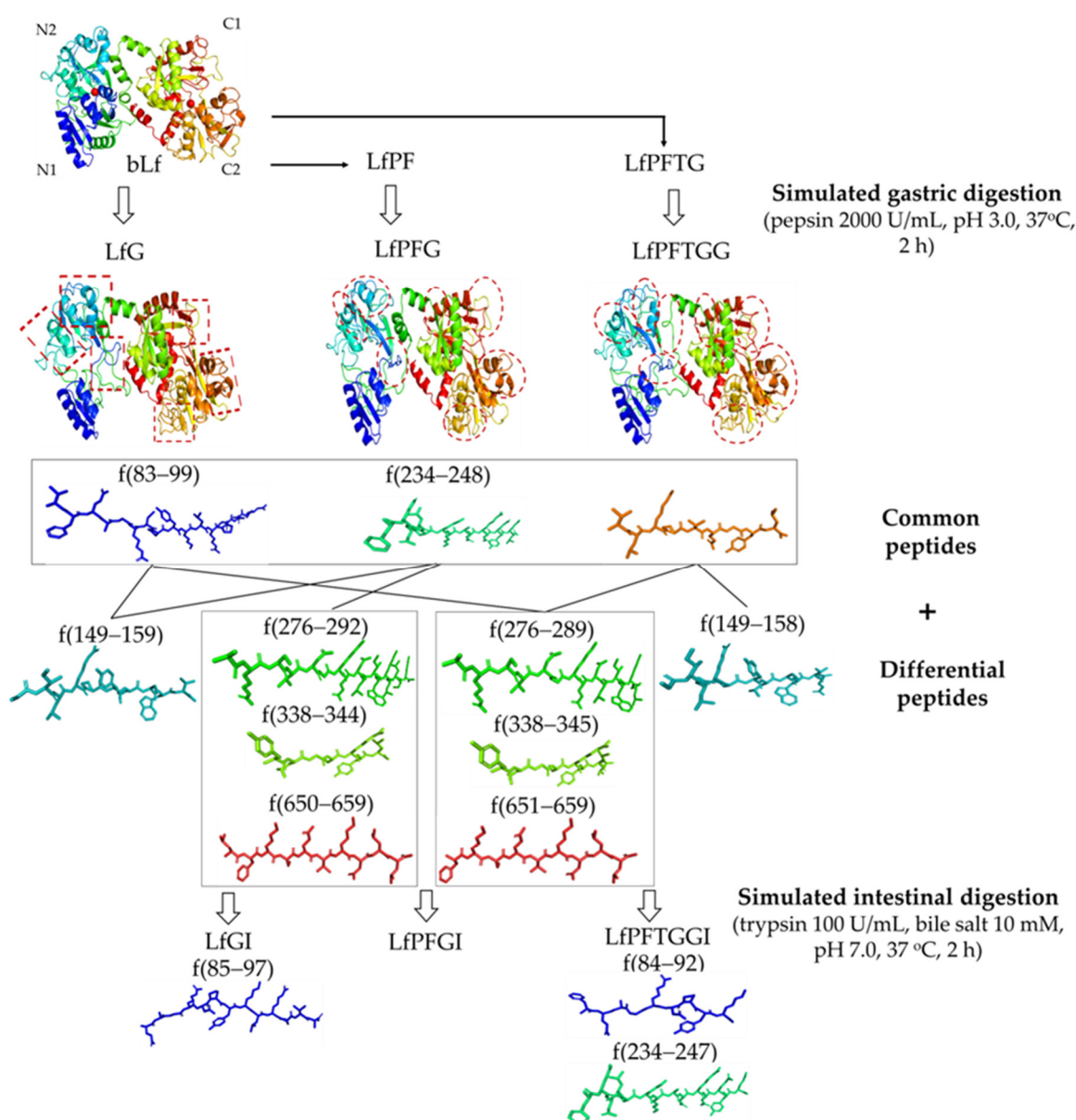


Figure 6. Active peptide production in the digests of bLf, LfPF complex, and LfPFTG complex during *in vitro* gastrointestinal digestion. Peptide fragments are in the same colors as in their parent bLf. Dashed frames indicate the action regions for pepsin.

3. Discussion

PP, as passion fruit low-methoxy pectin ($DE = 35.17\%$), exhibits lower GalA%, HG%, and linearity ratio, but greater RG-I%, degree of branching, and RG-I side chain length compared to its high-methoxy counterpart ($DE = 75.2\%$; GalA:Ara:Gal:Glc:Rha = 78.5:8.2:3.7:6.2:3.1; HG% = 74.3%; RG-I% = 18.1%; linearity ratio = 3.43; degree of branching = 0.04; RG-I side chain length = 3.9) [30]. In addition, PP displays similar GalA% and structural linearity, greater HG% and RG-I side chain length, but lower RG-I% and degree of branching when compared to citrus low-methoxy pectin ($DE = 38.2\%$; GalA:Ara:Gal:Glc:Rha = 52.0:0.6:31.0:9.0:7.4; HG% = 44.6%; RG-I% = 46.4%; linearity ratio = 1.33; degree of branching = 0.14; RG-I side chain length = 4.2 [19]. The TPC of the PF conjugate formed between PP and FA in this study (20 mg GAE/g) is almost double those (9.6–12.3 GAE mg/g) of passion fruit high-methoxy pectin–FA or caffeic acid conjugates [20] and citrus low-methoxy pectin–caffeic acid conjugate [19]. Briefly, the enhanced TPC for the PF conjugate could be attributed to two pectin structural features that facilitate the binding of phenolic acids: low DE (alternatively, high proportion of free carboxyl groups) and high RG-I side chain length.

The laccase-mediated formation of the PF conjugate involves mostly the formation of an ester linkage between the GalA C6 free carboxyl group and the FA moiety, as suggested by NMR spectra (Figure 1). The proposed mechanism includes FA oxidation catalyzed by laccase in the presence of O_2 to generate quinones with free radicals [31], which in turn undergo cross-linking reactions with free carboxyl groups in pectins [16,19]. Similar results are reported in the cases of gum Arabic [32] and proteins [31]. In this study, the laccase-mediated effect endowed the resultant PF conjugate with a higher DE and hydrophobicity, resulting in the given PF-encapsulated bLf complex of lessened particle sizes, greatedened total peptide yield, and longer peptides associated with higher peptide abundances in the digest LfPFG (Figure 5B), in contrast to bLf alone. The difference in peptide profile between LfPFG from LfG or LfPFTGG (Figure 5A–C) could be linked to PF interactions differentially with the N and C termini of bLf, since the N termini with positive charges [33] may interact with negatively charged PF more strongly than the C termini. However, more studies on the molecular mechanism for interactions between bLf and PF are necessary for understanding the controlled release of active bLf peptides by PF encapsulation approaches.

It is evident that seven types of active peptide fragments from bLf appeared in all gastric digests (LfG, LfPFG, and LfPFTGG) studied. The varieties of detected peptide fragments cover most of the bioactive peptides reported elsewhere. Accordingly, the sequences of bioactive peptide fragments reported are compared with those of the active peptide-related fragments in this study in Table 3. For antimicrobial peptides, bovine lactoferricin (bLfcin, f(17–41)) and lactoferrampin (bLfampin, f(268–288), f(271–288)) are well known, and bLfampin, rather than bLfcin, was identified in a digest using human gastric juice (pH 2.5) and duodenal juice (pH 7.0) [5]. The key sequences for antihypertensive bLf peptides discovered include the following: LIWKL, LFH, RPYL, and LNNSRAP fragments that are present in the gastric (pepsin) digest (pH 2.5, 4 h) of bLf [9]; ENLPEKADRD, present in the gastrointestinal (pepsin + trypsin) digest of bLf [6]; and LRP, DPYKLRP, PYKLRP, YKLRP, KLRP, and GILRP, present in the pepsin digest of Lf from yeast *Kluyveromyces marxianus* [29]. Osteoblast-promoting peptides of the sequences of ENLPEKADRDQYEL in the trypsin digest of bLf [7] and FKSETKNLL in the pepsin digest of bLf (pH 2.5, 4 h) [8] have been reported. In addition, the GSRY fragment, a sequence of potent SARS-CoV-2 inhibition, was found in the gastrointestinal (pepsin + trypsin) digest of bLf [34]. Accordingly, the peptides discovered comprising DGGMVFEAGRDPYKLRPVAAE, f(79–99); GILRPYLSWTE, f(149–159); YLGSRYLT, f(338–345); and VLRPTEGYL, f(445–453) (involving active fragments LRP, DPYKLRP, PYKLRP, YKLRP, YL, LRP, RPYL, or GILRP [29]), would be potent in antihypertensive activity as angiotensin-converting enzyme inhibitors (ACEIs). YLGSRYLT (containing GSRY) may be developed into a SARS-CoV-2 inhibitor. ARSVDGKEDLIWKLLSK, f(276–292), the fragment of bLfampin and composing antihypertensive fragment LIWKL [9], would be potent for antimicrobial and antihypertensive activities. FKSETKNLL and ENLPEKADRDQYEL are osteoblast-promoting peptides, as

reported [7,8]. Additionally, ENLPEKADRDQYEL is also reported to have anticoagulant activity [7]. The obtained digests possessing seven types of potentially active bLf peptides could be applied for multifunction nutraceuticals [1] or purified in advance for nonantibiotic therapeutic agents [2] or targeting antibacterial vaccines [35].

Table 3. Active peptide fragments from various lactoferrins reported and in this study.

Source	Digestion Conditions	Active Peptides	Reference
Bovine Lf	Human gastric juice (HGJ, pH 2.5); human duodenal juice (HDJ, pH 7.0)	Antimicrobial peptide: bLfampin f(268–288); no bLfcin, f(17–41), detected; 70% peptides from N terminus	[5]
Bovine Lf	Porcine pepsin (2540 U/mg, pH 2.5, 37 °C, 4 h)	Antihypertensive (ACE-inhibitory) peptides: LIWKL; LFH; RPYL; LNNSRAP	[9]
<i>Kluyveromyces marxianus</i> Lf	Pepsin (0.02 mg/mL, pH 2.0, 37 °C, 90 min)	Antihypertensive (ACE-inhibitory) peptides: LRP, DPYKLRP, PYKLRP, YKLRP, KLRP, GILRP	[29]
Bovine Lf	Porcine pepsin (1:100 w/w), pH 2.0, 37 °C, 90 min; porcine pancreatin (E/S = 1%), pH 7.4, 3 h	ACE inhibitor, anticoagulant peptide: ENLPEKADRD	[6]
Bovine Lf	Porcine trypsin (3 U/mg, pH 8.0, 37 °C, 2 h)	Osteoblast-promoting peptide: ENLPEKADRDQYEL	[7]
Bovine Lf	Porcine pepsin (3%, 2500 U/mg, pH 2.5, 37 °C, 4 h)	Osteoblast-promoting peptide: FKSETKNLL	[8]
Bovine Lf	Porcine pepsin (2000 U/mL, pH 3.0, 37 °C, 2 h)	DGGMVFEAGRDPYKLRPVAAE, GILRPYLSWTE, VLRPTEGYL, YLGSRYLT, ARSVDGKEDLIWKLLSK, FKSETKNLL, ENLPEKADRDQYEL	This study

In this study, Lfampin, rather than bLfcin, fragments were discovered in three gastric digests, implying that the Lfampin fragment is more resistant to gastric digestion than Lfcin is. The incorporation of PF resulted in the LfPFG having a diverse peptide distribution (Table 2), with more long peptides (Figure 5B), and a higher total peptide abundance (protein coverage rate = 37.5%, in contrast to 32.5% for LfG). This points to the protection of PF encapsulation on bLf against in vitro gastric digestion, consistent with the case of bLf complexes with citrus low-methoxy pectins [13,14]. The fact that LfPFTGGI exhibited more peptide fragments than LfGI and LfPFGI could be attributed to the presence of TG (5 U/mL in this study), potentially via γ -glutamyl-lysine (Gln-Lys) cross-links between polypeptide chains [21,22].

4. Materials and Methods

4.1. Materials and Reagents

Passion fruit pectin (PP) was extracted from purple passion fruit peel, by using 0.48% (w/v) citric acid aqueous solution at 80 °C for 2.5 h. Anhydrous citric acid, anhydrous ethanol, ferulic acid (FA), bovine lactoferrin (bLf) with iron saturation = 20.8%, and bovine bile salt (bile acid > 60%) were obtained from Adamas Reagent Co. (Basel, Switzerland). Trypsin from bovine pancreas (50 U/mg), γ -glutamyl transferase (transglutaminase, TG) from bovine kidney (≥ 5 U/mg), artificial gastric electrolyte, and intestinal electrolyte were from Shanghai Yuanye Biotechnology Co. (Shanghai, China). Arabinose (Ara), galactose (Gal), galacturonic acid (GalA), glucose (Glc), rhamnose (Rha), laccase (0.5 U/mg, from *Aspergillus* sp.), and porcine pepsin (≥ 250 U/mg) were obtained from Sigma-Aldrich Co. LLC (St. Louis, MO, USA). Pierce BCA protein assay kit, trifluoroacetic acid, acetonitrile (LC/MS grade), formic acid (LC/MS grade), methanol (LC/MS grade), and water (LC/MS grade) were from ThermoFisher Scientific (Shanghai, China).

4.2. Preparation of PP-FA Conjugate (PF)

The preparation of PF conjugate was performed according to the methods of Karaki et al. [17] and our previous studies [15,19]. Five grams of PP was well dissolved in 425 mL

phosphate buffer (50 mmol/L, pH 6.5) by heating (80 °C for 1 h) under stirring and cooling to room temperature. A portion of the given PP solution was then mixed with 0.2 mol/L ferulic acid (in anhydrous ethanol) at an equivalent volume, giving a final concentration of 1% (*w/w*) PP and 30 mmol/L FA (the molar ratio of free carboxy group on PP to FA = 1:1). The mixture was combined with 50 U laccase for reaction at 4 °C for 24 h in the dark. The sample was dialyzed (8–14 kDa) against deionized water for 48 h by refreshing water every other 6 h to remove free FA. The dialysate was concentrated in vacuo at ~55 °C and freeze-dried, yielding the PP-FA conjugate (namely PF).

4.3. Preparation of bLf-PF Complex (LfPF)

According to the results of our preliminary experiments and Niu et al. [14], the bLf preparation (0.2% (*w/w*), pH 5.5) was dissolved at ambient temperature under stirring (350 rpm) for 2 h. The PF preparation (0.05% (*w/w*)) was dissolved in distilled water at 50 °C for 30 min and further stirred at room temperature for 1 h. bLf and PF preparations were then mixed at 1:1 *v/v* and kept at 50 °C for 10 min under stirring (350 rpm) for the spontaneous formation of the polyelectrolytic complex (LfPF). In addition, the LfPF dispersion was further treated with TG (5 U/mL, 0.1% (*w/w*)) for 10 min under mild stirring (350 rpm) at room temperature, yielding the LfPFTG complex. The complex product was collected by centrifugation (12,500 × *g*, 10 min) to remove free bLf, followed by freeze-drying and storing in a desiccator before use.

4.4. Measurement of Uronic Acid Content

The uronic acid content assay was performed according to the *m*-hydroxybiphenyl method [36], using galacturonic acid (GalA) as a standard. The absorbance at 525 nm (A_{525}) of the reacted product was measured in a UV spectrophotometer (model 725, Shanghai Spectrum Instruments, Co., Ltd., Shanghai, China). The GalA content in the sample was derived by calibration with the standard curve of GalA: $y = 8.691x + 0.029$, $R^2 = 0.992$, where $y = A_{525}$ value and $x = \text{GalA concentration (0.01–0.09 mg/mL)}$. All data were examined in triplicate.

4.5. Determination of Total Phenolic Content

Total phenolic content was determined by referring to the method of Sato et al. [37], using gallic acid as a standard. The absorbance at 720 nm (A_{720}) of the reacted product was measured. Total phenolic content in the sample was determined by calibration with the gallic acid standard curve: $y = 0.038x - 0.004$, $R^2 = 0.996$, where $y = A_{720}$ value and $x = \text{gallic acid concentration (0.05–0.25 mg/mL)}$. The data were examined in triplicate and expressed as gallic acid equivalent (GAE) mg/g.

4.6. Measurement on Degree of Esterification

The degree of esterification (DE) was measured by titration with 0.05 mol/L NaOH, according to the method GB 25533-2010, National Food Safety Standard for food additive pectin, National Standard of People's Republic of China.

4.7. Assessment of Monosaccharide Composition

The sample (10 mg) was hydrolyzed with 0.2 mol/L trifluoroacetic acid (2 mL) at 110 °C for 2 h. The hydrolysate was successively cooled to room temperature, dried with nitrogen flux to remove trifluoroacetic acid, washed with methanol thrice, dissolved in 2 mL deionized (18.25 M Ω ·cm) water, microfiltered (0.22 μm), and subjected to high-performance anion exchange chromatography (HPAEC). A Thermo ICS-5000+ HPAEC (ThermoFisher Scientific Inc., Waltham, MA, USA) coupled with a PAD detector and guarded CarboPac PA20 analytic column (150 mm × 3 mm) (Dionex Co., Sunnyvale, CA, USA) at 30 °C was applied. The mobile phase was the mixture of four solutions: (A) deionized (18.25 M Ω ·cm) water; (B) 25 mmol/L NaOH aqueous solution; (C) 1 mol/L sodium acetate aqueous solution; and (D) 200 mmol/L NaOH. The elution program for analysis was as follows: 0–20 min, A 75% + B 25%; 20.1 min, A 70% + B 25% + C 5%; 30 min, A 55% + B 25% + C 20%.

in linear gradient. The elution rate was 0.5 mL/min. The injection volume of the sample was 25 μ L. Data acquisition and processing and chromatographic analysis were managed with Chromeleon 7 software (ThermoFisher Scientific Inc., Waltham, MA, USA). The monosaccharide composition of the sample was quantified by calibration with monosaccharide standard curves: Ara: $y = 2098x + 1.481$, $R^2 = 0.992$; Rha: $y = 842.5x + 0.494$, $R^2 = 0.996$; Gal: $y = 1490x + 1.313$, $R^2 = 0.998$; Glc: $y = 1200x + 2.448$, $R^2 = 0.993$; GalA: $y = 1261x + 0.031$, $R^2 = 1.000$, where y = peak area (nC·min, nC = PAD detector signal) and x = monosaccharide concentration (1.25~12.5 μ g/mL).

4.8. Nuclear Magnetic Resonance (NMR) Analysis

The pectin sample (40 mg) was subjected to H-D exchange by dissolving it in 1 mL of D₂O and freeze-drying it, and the procedure was repeated three times. The sample was then fully dissolved in 1 mL of D₂O and transferred to a 5 mm NMR dual tube. A 700 MHz AVANCE NEO NMR spectrometer (Bruker, Karlsruhe, Germany) was used to acquire 700.23 MHz ¹H-decoupled and 176.07 MHz ¹³C spectra at 298.0 K. The spectral width, acquisition time, and scan number were 14.7 kHz, 1.114 s, and 128 for ¹H-decoupled spectra and 41.7 kHz, 0.393 s, and 3000 for ¹³C spectra, respectively. The chemical shifts (δ) were expressed as parts per million (p.p.m.) in reference to external standard tetramethylsilane (TMS).

4.9. Examination of Particle Size Distribution

Particle size distribution of sample solution was assayed using a multiangle light scattering particle size analyzer (model 173 plus, Brookhaven Instrument Co., Holtsville, NY, USA) at an angle of 90° for a detection time of 120 s after equilibrium for 120 s at room temperature. Effective particle size was obtained with Particle Solution software. All data were measured in three replications.

4.10. ζ -Potential Analysis

The ζ -potential value of the sample solution was determined using a Zetasizer Nano ZS (Malvern Instruments Ltd., Malvern, UK). All data were measured in three replications.

4.11. Digestomics Analysis

4.11.1. In Vitro Simulated Gastrointestinal Digestion

Experimental conditions for in vitro simulated gastrointestinal digestion were mainly established according to the method of Minekus et al. [38] with slight modifications. A portion of bLf or its complex sample (10 mg/mL in deionized water, 10 mL) was mixed with concentrated artificial gastric electrolyte at 1:1 (v/v), followed by successively adjusting pH to 3.0 with diluted NaOH aqueous solution and adding CaCl₂ to a final concentration of 0.15 mmol/L CaCl₂ and pepsin to a final pepsin activity of 2000 U/mL. The mixture was kept at 37 °C for 2 h under shaking (95 rpm) for digestion, followed by centrifugation (2599 \times g , 5 min) at 4 °C to give the supernatant. The supernatant was lyophilized and stored at −18 °C for peptide identification.

For in vitro simulated intestinal digestion, a fresh supernatant of the gastric digest was mixed with concentrated simulated intestinal electrolyte at 1:1 (v/v), followed by consecutively adjusting pH to 7.0, adding bile salt solution to 10 mmol/L, mixing well, adding 0.04 mL CaCl₂ aqueous solution to 0.6 mmol/L CaCl₂, and adding bovine trypsin solution to 100 U/mL. The mixture was kept at 37 °C for 2 h under shaking (95 rpm) for digestion. The resultant digest was centrifuged (6654 \times g , 15 min) at 4 °C, yielding the supernatant for lyophilization and storage at −18 °C before peptide identification.

4.11.2. Peptide Purification

The lyophilized digested sample was dissolved in a portion of 8 mol/L urea, followed by microfiltration (molecular weight cut off = 10 kDa) to remove undigested residues and freeze-drying. The sample was successively re-dissolved in 0.1% (w/w) trifluoroacetic acid aqueous solution, desalted on an Oasis HLB 96-Well Plate column (30 μ m) (Waters Co.,

Shanghai, China), freeze-dried, completely re-dissolved in the aqueous solution containing 50% (*v/v*) acetonitrile and 0.5% (*v/v*) trifluoroacetic acid, re-desalted on an Oasis MCX μ Elution Plate column (30 μ m) (Waters Co., Shanghai, China), and freeze-dried. The resultant purified sample was detected for total peptide content using the Pierce BCA protein assay kit (ThermoFisher Scientific Co., Ltd.) and bovine serum albumin for the standard curve ($y = 2.025x + 0.720$, $R^2 = 0.999$, y = the absorbance at 480 nm, $x = 0.125$ – 1.00 μ g/ μ L). The yield of total purified peptides was calculated on the basis of 100 mg bLf or its complex applied for gastrointestinal digestion.

4.11.3. UPLC-MS-MS Analysis for Peptide Distribution

According to total peptide content, sample solution (0.25 μ g peptide/ μ L) was prepared in the aqueous solvent containing 2% (*v/v*) acetonitrile and 0.1% (*v/v*) formic acid for UPLC-MS-MS analysis. An EASY-nLC 1200 UPLC system coupled with a C18 column (75 μ m \times 25 cm, Thermo Scientific) and Q Exactive HF-X mass spectrometer (Thermo Scientific, Waltham, MA, USA) was employed. The elution was performed by mixing aqueous solutions A (2% acetonitrile + 0.1% formic acid) and B (80% acetonitrile + 0.1% formic acid) according to the following gradient program: 0 min, 5% B; 34 min, 23% B; 39 min, 29% B; 41 min, 38% B; 43–60 min, 100% B; linear gradient. The elution rate was 300 nL/min. Data were collected and managed with Thermo Xcalibur 4.0 software (Thermo Scientific).

For mass spectrometry, the MS scanning range (m/z) was 300–1500, and the acquisition mode was DDA. The primary fragments of the 20 strongest signals were subjected to secondary fragmentation. The conditions for primary fragmentation were as follows: resolution, 60,000; AGC target, 3×10^6 ; maximal injection time, 20 ms; fragmentation mode, HCD. For secondary fragmentation, the conditions were as follows: resolution, 15,000; AGC target, 1×10^5 ; maximum injection time, 50 ms; fixed first mass, 100 m/z ; minimal AGC target, 8000; intensity threshold: 1.6×10^5 ; dynamic exclusion time, 18 s.

4.11.4. Homology Matching and Molecular Modeling

The obtained MS data were exported to the UniProt Knowledgebase (<https://www.uniprot.org/uniprotkb/P24627/entry>, accessed on 20 September 2022) and SWISS-MODEL (Swiss Institute of Bioinformatics, <https://swissmodel.expasy.org/>, accessed on 22 September 2022) for homology matching using PEAKS Studio 8.5 server and based on the amino acid sequence of bLf retrieved from UniProt Knowledgebase. The bLf 3D model was built by using SWISS-MODEL. Peptide 3D models were created using PyMol 2.3.0 (Schrödinger, New York, NY, USA).

4.12. Statistical Analysis

Significant differences between data at $p < 0.05$ were assessed by one-way analysis of variance (ANOVA) using SPSS software 25.0 (SPSS Inc., Chicago, IL, USA). OriginPro 2021b (Origin Lab, Northampton, MA, USA) was applied for plotting.

5. Conclusions

In this study, 103 bLf peptide fragments identified by UPLC-MS-MS, including seven groups of active peptide fragments, were obtained by using conditioned *in vitro* gastric digestion (pepsin activity 2000 U/mL, pH 3.0, 37 °C, 2 h). The discovered active peptide fragments related to three common active peptides (VFEAGRDPYKLRPVAE, FENLPEKADRDQYEL, and VLRPTEGYL) and four differential active peptides (GILRPYL-SWTE, ARSVDGKEDLIWKL, YLGSRYLT, and FKSETKNLL). Encapsulation by laccase-mediated pectin–ferulic acid conjugate (PF) improved the diversity, abundances, and long-chain species of bLf peptide fragments (including active peptides) in the gastric digest. Differently, moderate TG treatment on LfPF facilitated active peptides FENLPEKADRDQYE and FEAGRDPYK remaining in the final gastrointestinal digest. The LfPFG digest containing seven types of potentially active bLf peptides with enhanced abundances is of great

potential for multipurpose use in nutraceuticals, clinical therapy, or targeting antibacterial vaccines. Based on the flow chart suggested for the production of active peptide fragments from bLf and its complexes with PF, more studies on cost-effective processes for isolating diverse bLf active peptides from the gastric digest are necessary for industrial applications. In addition, the optimal TG concentration and action sites for TG-induced crosslinking between bLf chains are interesting and under investigation.

Supplementary Materials: The following supporting information can be downloaded at: <https://www.mdpi.com/article/10.3390/catal13030521/s1>, Table S1: UPLC-MS-MS-identified molecular information for all peptide fragments in the digests of Lf, LfPF complex, and LfPFTG complex; Table S2: Peptide fragments found in the digests of Lf, LfPF complex, and LfPFTG complex.

Author Contributions: M.X.: Methodology, Investigation, Formal Analysis, Data Curation, Writing—Original Draft; Y.J.: Methodology, Investigation, Formal Analysis; L.A.: Supervision, Funding Acquisition, Review and Editing; F.X.: Methodology, Project Administration, Review and Editing; Y.W.: Funding Acquisition, Review and Editing; P.F.H.L.: Conceptualization, Supervision, Validation, Data Curation, Writing—Review and Editing. All authors have read and agreed to the published version of the manuscript.

Funding: This work was supported by Shanghai Science and Technology Development Fund, Domestic Science and Technology Cooperation Project (Grant No.: 21015800300).

Data Availability Statement: UPLC-MS-MS-identified information for peptides is available in the Supplementary Materials.

Acknowledgments: The authors thank Shanghai Majorbio Bio-pharm Technology Co., Ltd., Shanghai, China, for technical help in UPLC-MS-MS analysis and peptide identification.

Conflicts of Interest: The authors declare that they have no known competing financial interests.

References

1. Iglesias-Figueroa, B.F.; Espinoza-Sánchez, E.A.; Siqueiros-Cendón, T.S.; Rascón-Cruz, Q. Lactoferrin as a nutraceutical protein from milk, an overview. *Int. Dairy J.* **2019**, *89*, 37–41. [[CrossRef](#)]
2. Elzoghby, A.O.; Abdelmoneem, M.A.; Hassanin, I.A.; Abd Elwakil, M.M.; Elnaggar, M.A.; Mokhtar, S.; Fang, J.-Y.; Elkhodalry, K.A. Lactoferrin, a multi-functional glycoprotein: Active therapeutic, drug nanocarrier & targeting ligand. *Biomaterials* **2020**, *263*, 120355. [[PubMed](#)]
3. Ji, Y.; Ai, L.Z.; Xing, M.X.; Xie, F.; Lai, P. Advances in research on bovine lactoferrin-based technical innovation and application. *Food Ferment. Ind.* **2022**, *48*, 332–340. [[CrossRef](#)]
4. Agwa, M.M.; Sabra, S. Lactoferrin coated or conjugated nanomaterials as an active targeting approach in nanomedicine. *Int. J. Biol. Macromol.* **2021**, *167*, 1527–1543. [[CrossRef](#)]
5. Furlund, C.B.; Ulleberg, E.K.; Devold, T.G.; Flengsrud, R.; Jacobsen, M.; Sekse, C.; Holm, H.; Vegarud, G.E. Identification of lactoferrin peptides generated by digestion with human gastrointestinal enzymes. *J. Dairy Sci.* **2013**, *96*, 75–88. [[CrossRef](#)] [[PubMed](#)]
6. Tu, M.; Xu, S.; Xu, Z.; Cheng, S.; Wu, D.; Liu, H.; Du, M. Identification of dual-function bovine lactoferrin peptides released using simulated gastrointestinal digestion. *Food Biosci.* **2021**, *39*, 100806. [[CrossRef](#)]
7. Shi, P.; Liu, M.; Fan, F.; Chen, H.; Yu, C.; Lu, W.; Du, M. Identification and mechanism of peptides with activity promoting osteoblast proliferation from bovine lactoferrin. *Food Biosci.* **2018**, *22*, 19–25. [[CrossRef](#)]
8. Shi, P.; Fan, F.; Chen, H.; Xu, Z.; Cheng, S.; Lu, W.; Du, M. A bovine lactoferrin-derived peptide induced osteogenesis via regulation of osteoblast proliferation and differentiation. *J. Dairy Sci.* **2020**, *103*, 3950–3960. [[CrossRef](#)]
9. Ruiz-Giménez, P.; Salom, J.B.; Marcos, J.F.; Vallés, S.; Martínez-Maqueda, D.; Recio, I.; Torregrosa, G.; Alborch, E.; Manzanares, P. Antihypertensive effect of a bovine lactoferrin pepsin hydrolysate: Identification of novel active peptides. *Food Chem.* **2012**, *131*, 266–273. [[CrossRef](#)]
10. Picariello, G.; Mamone, G.; Nitride, C.; Addeo, F.; Peranti, P. Protein digestomics: Integrated platforms to study food-protein digestion and derived functional and active peptides. *TrAC-Trend Anal. Chem.* **2013**, *52*, 120–134. [[CrossRef](#)]
11. Basak, S.; Annature, U.S. Trends in “green” and novel methods of pectin modification—A review. *Carbohydr. Polym.* **2022**, *278*, 118967. [[CrossRef](#)]
12. Li, D.-q.; Li, J.; Dong, H.-l.; Li, X.; Zhang, J.-q.; Ramaswamy, S.; Xu, F. Pectin in biomedical and drug delivery applications: A review. *Int. J. Biol. Macromol.* **2021**, *185*, 49–65. [[CrossRef](#)] [[PubMed](#)]
13. Bengoechea, C.; Jones, O.G.; Guerrero, A.; McClements, D.J. Formation and characterization of lactoferrin/pectin electrostatic complexes: Impact of composition, pH and thermal treatment. *Food Hydrocoll.* **2011**, *25*, 1227–1232. [[CrossRef](#)]

14. Niu, Z.; Loveday, S.M.; Barbe, V.; Thielen, I.; He, Y.; Singh, H. Protection of native lactoferrin under gastric conditions through complexation with pectin and chitosan. *Food Hydrocoll.* **2019**, *93*, 120–130. [CrossRef]
15. Ji, Y. Study on Preparation Technology, Formulation Optimization and Active Peptide of Lactoferrin-Pectin Complex. Master Thesis, University of Shanghai for Science & Technology, Shanghai, China, 2022.
16. Karaki, N.; Aljawish, A.; Muniglia, L.; Humeau, C.; Jasniewski, J. Physicochemical characterization of pectin grafted with exogenous phenols. *Food Hydrocoll.* **2016**, *60*, 486–493. [CrossRef]
17. Karaki, N.; Aljawish, A.; Muniglia, L.; Bouguet-Bonnet, S.; Leclerc, S.; Paris, C.; Jasniewski, J. Functionalization of pectin with laccase-mediated oxidation products of ferulic acid. *Enz. Microbial Technol.* **2017**, *104*, 1–8. [CrossRef] [PubMed]
18. Robert, B.; Chenthamara, D.; Subramaniam, S. Fabrication and biomedical applications of arabinoxylan, pectin, chitosan, soyprotein, and silk fibroin hydrogels via laccase—Ferulic acid redox chemistry. *Int. J. Biol. Macromol.* **2022**, *201*, 539–556. [CrossRef]
19. Gao, F.; Ai, L.Z.; Wu, Y.; Lai, F.X.; Zhang, H.; Xie, F.; Song, Z.B. Structural mechanism and structure-antioxidant activity relationship of low-methoxyl pectin-caffeic acid conjugate. *Food Sci.* **2022**, *43*, 19–29.
20. Gao, F.; Ding, N.; Ai, L.; Lai, P.; Zhang, H.; Song, Z. Molecular characteristics, in vitro antioxidant and immunological activities of high-methoxy pectin-phenolic acid derivatives from passion fruit. *Food Sci.* **2022**, *43*, 84–94. Available online: <https://www.spkx.net.cn/article/2022/1002-6630/2022-43-17-010.html> (accessed on 20 September 2022).
21. Miwa, N. Innovation in the food industry using microbial transglutaminase: Keys to success and future prospects. *Anal. Biochem.* **2020**, *597*, 113638. [CrossRef]
22. Xia, T.; Gao, Y.; Liu, Y.; Wei, Z.; Xue, C. Lactoferrin particle assembled via transglutaminase-induced crosslinking: Utilization in oleogel-based Pickering emulsions with improved curcumin bioaccessibility. *Food Chem.* **2022**, *374*, 131779. [CrossRef] [PubMed]
23. Martini, S.; Solieri, L.; Tagliacruzchi, D. Peptidomics: New trends in food science. *Curr. Opin. Food Sci.* **2021**, *39*, 51–59. [CrossRef]
24. Lin, Y.; An, F.; He, H.; Geng, F.; Song, H.; Huang, Q. Structural and rheological characterization of pectin from passion fruit (*Passiflora edulis f. flavicarpa*) peel extracted by high-speed shearing. *Food Hydrocoll.* **2021**, *114*, 106555. [CrossRef]
25. Cui, L.; Wang, J.; Huang, R.; Tan, Y.; Zhang, F.; Zhou, Y.; Sun, L. Analysis of pectin from Panax ginseng flower buds and their binding activities to galactin-3. *Int. J. Biol. Macromol.* **2019**, *128*, 459–467. [CrossRef]
26. Liu, D.; Zhai, L.-Y.; Shi, Z.-H.; Hong, H.-L.; Liu, L.-Y.; Zhao, S.-R.; Hu, Y.-B. Purification and fine structural analysis of pectin polysaccharides from *Osmunda Japonica Thunb.* *J. Mol. Struct.* **2022**, *1269*, 133828. [CrossRef]
27. De Cicco, M.; Mamone, G.; Di Stasio, L.; Ferranti, P.; Addeo, F.; Picariello, G. Hidden “digestome”: Current analytical approaches provide incomplete peptide inventories of food digests. *J. Agr. Food Chem.* **2019**, *67*, 7775–7782. [CrossRef] [PubMed]
28. Nielsen, S.D.; Beverly, R.L.; Qu, Y.; Dallas, D.C. Milk bioactive peptide database: A comprehensive database of milk protein-derived bioactive peptides and novel visualization. *Food Chem.* **2017**, *232*, 673–682. [CrossRef]
29. García-Tejedor, A.; Castelló-Ruiz, M.; Gimeno-Alcañiz, J.V.; Manzanares, P.; Salom, J.B. In vivo antihypertensive mechanism of lactoferrin-derived peptides: Reversion of angiotensin I- and angiotensin II-induced hypertension in Wistar rats. *J. Funct. Foods* **2015**, *15*, 294–300. [CrossRef]
30. Ding, N. Study on Extraction of Passion Fruit Peel Pectin, Derivatization and Functionality. Master Thesis, University of Shanghai for Science & Technology, Shanghai, China, 2020.
31. Li, X.; Li, S.; Liang, X.; McClements, D.J.; Liu, X.; Liu, F. Applications of oxidases in modification of food molecules and colloidal systems: Laccase, peroxidase and tyrosinase. *Trends Food Sci. Tech.* **2020**, *103*, 78–93. [CrossRef]
32. Vuillemin, M.E.; Muniglia, L.; Linder, M.; Bouguet-Bonnet, S.; Poinsignon, S.; Morais, R.D.S.; Simard, B.; Paris, C.; Michaux, F.; Jasniewski, J. Polymer functionalization through an enzymatic process: Intermediate products characterization and their grafting onto gum Arabic. *Int. J. Biol. Macromol.* **2021**, *169*, 480–491. [CrossRef]
33. Moreno-Expósito, L.; Illescas-Montes, R.; Melguizo-Rodríguez, L.; Ruiz, C.; Ramos-Torrecillas, J.; de Luna-Bertos, E. Multifunctional capacity and therapeutic potential of lactoferrin. *Life Sci.* **2018**, *195*, 61–64. [CrossRef] [PubMed]
34. Zhao, W.; Li, X.; Yu, Z.; Wu, S.; Ding, L.; Liu, J. Identification of lactoferrin-derived peptides as potential inhibitors against the main protease of SARS-CoV-2. *LWT* **2022**, *154*, 112684. [CrossRef] [PubMed]
35. Schryvers, A.B. Targeting bacterial transferrin and lactoferrin receptors for vaccines. *Trends Microbiol.* **2022**, *30*, 820–830. [CrossRef] [PubMed]
36. Blumenkrantz, N.; Hansen, G.A. New method for quantitative determination of uronic acids. *Anal. Biochem.* **1973**, *54*, 484–489. [CrossRef]
37. Sato, M.; Ramarathnam, N.; Suzuki, Y.; Ohkubo, T.; Takeuchi, M.; Ochi, H. Varietal differences in the phenolic content and superoxide radical scavenging potential of wines from different sources. *J. Agr. Food Chem.* **1996**, *44*, 37–41. [CrossRef]
38. Minekus, M.; Alvinger, M.; Alvito, P.; Balance, S.; Bohn, T.; Bourlieu, C.; Carrière, F.; Boutrou, R.; Corredig, M.; Dupont, D.; et al. A standardised static in vitro digestion method suitable for food—an international consensus. *Food Funct.* **2014**, *5*, 1113–1124. [CrossRef] [PubMed]

Disclaimer/Publisher’s Note: The statements, opinions and data contained in all publications are solely those of the individual author(s) and contributor(s) and not of MDPI and/or the editor(s). MDPI and/or the editor(s) disclaim responsibility for any injury to people or property resulting from any ideas, methods, instructions or products referred to in the content.